Food Chemistry 115 (2009) 304–312

Contents lists available at ScienceDirect

Food Chemistry

journal homepage: www.elsevier.com/locate/foodchem

Analytical Methods

Rapid assessment of neoformed compounds in nuts and sesame seeds by front-face fluorescence

Rita Yaacoub [a,c,*], Rachad Saliba [b], Bilal Nsouli [a], Gaby Khalaf [a], Jad Rizkallah [c], Inès Birlouez-Aragon [c]

[a] Lebanese Atomic Energy Commission, National Council for Scientific Research, Airport Highway, Riad El Solh 1107 2260 Beirut, Lebanon
[b] Department of Agro- Food science and Technology, Faculty of Agriculture Sciences, Lebanese University, Lebanon
[c] AgroParisTech, F-75231, Paris Cedex 05, France

ARTICLE INFO

Article history:
Received 16 June 2008
Received in revised form 3 September 2008
Accepted 16 November 2008

Keywords:
Fluorescence
PARAFAC
Nuts
Sesame seeds
Lipid oxidation
Carboxymethyllysine
Trans fatty acids

ABSTRACT

The potential of a rapid spectral method, based on front-face fluorescence, to monitor lipid neoformed compounds (NFC) during processing of nuts and sesame seeds was investigated. Fluorescence fingerprints were obtained from front-face fluorescence acquisition directly on crushed nuts and sesame seed samples obtained at different stages of processing. Fluorescence was very sensitive to physicochemical changes induced by the heat process, namely roasting. Parallel factor (PARAFAC) analysis of the fluorescence landscapes revealed four main fluorescence profiles in the nuts, and five in the sesame seeds. These were associated with peptidic tryptophan, tocopherols and process derived products. Various regression models between fluorescence spectra and NFC appearing during the process, carboxymethyllysine (CML) and *trans* fatty acids (tFA) showed good correlations ($R > 0.89$) and satisfactory prediction errors (RMSECV < 1.67). When applied to indicators of lipid peroxidation, good regression models were also obtained allowing prediction of the *p*AV (*p*-anisidine value) and TBARs (thiobarbituric acid reactive substances): $R = 0.73$ and 0.96 in nuts and sesame seeds, respectively, with prediction errors lower than 0.78. This study demonstrates the interest of front-face fluorescence as a promising tool for quality control of nuts and seeds roasting.

1. Introduction

Foods are complex mixtures of chemical constituents which interact during processing leading to oxidation and glycation reactions upon heating. Nuts and sesame seeds are particularly rich in both lipids and proteins; making them very susceptible to oxidation and Maillard reactions during thermal treatment. Consequently, loss of nutritional value, changes in the organoleptic quality and accumulation of NFC (oxidized lipids, *trans* fatty acids and carboxymethyllysine) with possible hazardous biological effects are commonly observed. The growing need for rigorously controlling the nutritional quality and safety of food products, together with the constraints associated with time consuming and expensive conventional methods, have led to a major need for reliable, rapid and non-invasive methods to evaluate Maillard reaction and lipid oxidation progress. In this context, fluorescence spectroscopy seems a promising technique due to its high sensitivity to food physicochemical changes resulting from industrial processing, and particularly suitable to monitor such changes (Rizkallah, Lakhal, & Birlouez-Aragon, 2008). Actually heat treatment applied to food samples induces many changes which strongly impact the global fluorescence fingerprint of the food matrix: on the one hand a decrease in the native fluorescence, due to degradation of some fluorescent constituents (tocopherols and phenols) (Cheikhousman et al., 2005) or modification of their physical environment (tryptophan) (Dufour & Riaublanc, 1997); and on the other hand, a development of neoformed fluorophores, essentially derived from the Maillard reaction (Birlouez-Aragon, Locquet, De St Louvent, Jouan-Rimbaud Bouveresse, & Stahl, 2005) or from lipid oxidation (Liang, 2000).

Several authors have demonstrated that fluorescence is a good indicator of lipid oxidation in food systems. Numerous fluorophores have been obtained following reactions between primary and secondary lipid peroxidation products and primary amines, and a majority of the unsaturated aldehydes formed by lipid peroxidation have been found to be precursors of fluorescent compounds (Esterbauer, Koller, Slee, & Koster, 1986; Melton, 1983). Through investigations on formation of fluorescent oxidation products, a variety of excitation and emission peaks have been reported

Abbreviations: CML, carboxymethyllysine; EEM, excitation emission matrix; FA, fatty acids; MLR, multiple linear regression; NFC, neoformed compounds; PARAFAC, parallel factor; *p*AV, *p*-anisidine value; PLS, partial least squares; RMSEC, root mean square error of calibration; RMSECV, root mean square error of cross validation; TBARS, thiobarbituric acid reactive substances; tFA, *trans* fatty acids.

* Corresponding author. Address: Lebanese Atomic Energy Commission, National Council for Scientific Research, Airport Highway, Riad El Solh 1107 2260 Beirut, Lebanon.
E-mail address: ritayaacoub@hotmail.com (R. Yaacoub).

0308-8146/$ - see front matter © 2008 Elsevier Ltd. All rights reserved.
doi:10.1016/j.foodchem.2008.11.104

(Hasegawa, Endo, & Fujimoto, 1992; Kikugawa & Beppu, 1987; Wold & Mielnik, 2000). Fluorescence has been shown as a high sensitive technique for detection of lipid oxidation in pork fat and poultry meat (Olsen, Vogt, Veberg, Ekeberg, & Nilsson, 2005; Wold, Mielnik, Pettersen, Aaby, & Baardseth, 2002), fish (Aubourg, 1999), processed cheese (Christensen, Povlsen, & Sorensen, 2003), milk powders (Liang, 2000), peanuts, oatmeal and muesli (Jensen, Christensen, & Engelsen, 2004), parma ham (Moller, Parolari, Gabba, Christensen, & Skibsted, 2003) and extra virgin olive oil (Cheikhousman et al., 2005). Fluorescence spectroscopy has also found applicability in monitoring frying oil deterioration by prediction of anisidine values, iodine values and vitamin E (Engelsen, 1997).

Fluorescence has been also used to evaluate the progress of Maillard reaction resulting from thermal treatment of milk (Birlouez-Aragon, Leclère, Ouedraogo, Birlouez, & Grongnet, 2001; Kulmyrzaev & Dufour, 2002) and infant formulas (Birlouez-Aragon et al., 2005).

Front-face fluorescence, which does not require any sample preparation, was applied to many food products, including cereal products, poultry meat, milk samples and vegetable oils, to directly monitor the heat process applied or to predict some indicators of the heat treatment (Birlouez-Aragon et al., 2004).

The approach of monitoring oxidation and Maillard products by using front-face spectroscopy is rather novel, and to the best of our knowledge, no such investigations were carried out on sesame seeds, or few on nuts. This paper explores the potential of fluorescence data analysis for predicting quality parameters related to deterioration of lipid rich foods, such as nuts and sesame. In the present study, nuts and sesame seed samples obtained from different stages of manufacture processing were analysed by front-face fluorescence spectroscopy directly applied on the samples. The underlying fluorescence structure of the fluorescence landscapes was investigated using PARAFAC model. Based on these data, we investigated (1) the potential of front-face fluorescence as a global approach to monitor the physicochemical changes induced by processing; (2) the potential of front-face fluorescence to predict CML and tFA content quantified by chromatographic methods; (3) the suitability of front-face fluorescence for predicting the lipid oxidation process assessed by hydroperoxides, TBARS and *p*AV.

2. Materials and methods

2.1. Samples and processing conditions

Three types of roasted nuts (almonds and peanuts) commonly consumed in Lebanon and sesame seed products (Tahina) were sampled at different steps of processing in the industrial plant of most representative local manufacturers. The products were processed according to the following manufacturing stages: (1) in nuts: stages A–D (A, raw material; B, roasting; C, seasoning; D, commercial end-product), and (2) in Tahina: stages A–I (A, raw material; B, soaking in water; C, dehulling; D, soaking in brine; E, drying; F and G, roasting (F: after 15 min of roasting, G: after 2 h of roasting); H, milling; I, sterilized end-product). At the level of the sesame seed roasting step (F), samples were collected every 15 min at three different places of the roaster to take into account the possible heterogeneity of the roaster. Peanuts and almonds were roasted at 180 °C for 10 min and 180 °C for 8 min, respectively.

2.1.1. Manufacture of Tahina

The sesame seeds were sieved then soaked in water for 2 h. The soaked seeds were stained off and passed through a peeler. The hulls and other foreign materials were separated by soaking in brine (180–200 g/l). The seeds were stained off and washed with water to remove the salt. The seeds were then left to dry at ambient temperature and passed through a roaster (115 °C for 2 h) (steam heated jacketed open drum with continuous stirring). The roasted sesame seeds were then sieved and ground by stone mills to a viscous paste which was sterilized (100 °C for 30 min), then filled into plastic containers and marketed as Tahina.

2.2. Analysis of chemical indicators by conventional methods

2.2.1. Hydroperoxides

Hydroperoxides were analysed by an indirect colorimetric method (Jiang, Woollard, & Wolff, 1990) based on the oxidation of iron(II) to iron(III) by hydroperoxides and subsequent formation of a brown chromophore in the presence of xylenol orange. 100 mg ± 5 mg of oil extract were diluted in 10 ml propanol-1, then 2400 μl of this solution was mixed with 600 μl of a methanolic reaction mixture of xylenol orange and iron(II) sulphate in H_2SO_4 (94%) and BHT (1%), before reaction for 30 min at room temperature. The solution was filtered through a nylon filter (Cluzeau) before reading the absorbance at 560 nm using a Unicam UV–vis spectrophotometer. Quantification used a calibration curve using H_2O_2. Results are expressed as mmol hydroperoxides per 100 mg fat.

2.2.2. p-Anisidine value (pAV)

Three hundred microlitre of oil extract diluted in propanol (10/90, v/v) was mixed with 1.9 ml *p*-anisidine solution in propanol (0.039 mol/l) and 0.7 ml glacial acetic acid. Absorbance was measured at 350 nm using a Unicam UV–vis spectrophotometer. *p*AV is defined as 100 times the absorbance measured at 350 nm.

2.2.3. Thiobarbituric acid reactive substances (TBARS)

TBARS values were determined using the TBA method described by Genot (1996). For extraction, 2 g of the sample was homogenised together with 16 ml of a 5% (w/v) aqueous solution of trichloroacetic acid (TCA) containing 100 μL of freshly prepared BHT in ethanol (1 mg/ml) by using a homogenizer set at 20,000 rpm for 15 s. After filtration, 2 ml extract was mixed with 2 ml of TBA (20 mol/l) in stoppered test tubes, and immersed in a 70 °C water bath for 30 min. After cooling, absorbance of the reaction solutions was read at 532 nm using a Unicam UV–vis spectrophotometer against a blank containing 2 ml of TCA and 2 ml of TBA reagent. Results are expressed as mg MDA per kg (or ppm) of food sample using a molar extinction coefficient of $1.56.10^5\ M^{-1}\ cm^{-1}$ for malondialdehyde (Buedge & Aust, 1978).

2.2.4. Chemical determination of CML

CML was quantified in the acid hydrolysed samples, after their derivatization using the method validated by Charissou, Ait-Ameur, and Birlouez-Aragon (2007). The CML was quantified by selected ion monitoring using a FOCUS GC (Thermo Electron Corporation) gas chromatograph coupled to a PolarisQ ion trap mass detector. The injection was made in the split mode at 250 °C. A 30 m × 0.25 mm × 0.25 μm DB5-MS capillary column was used. The temperature program was as follows: initial temperature, 70 °C (2 min holding), raised to 260 °C at 5 °C/min and further to 290 °C at 15 °C/min, then isothermal for 5 min. The carrier gas was helium at a flow rate of 1.5 ml/min. The mass spectrometer was operated in the electron impact mode at 70 eV. The $m/z = 392$ as a parent ion was isolated using an energy = 0.90 V. The ions generated were: 374 (25%), 360 (100%), 332 (40%) and 206 (10%). Data were collected and integrated with Xcalibur software (Thermo Electron Corporation).

2.2.5. Chemical determination of trans fatty acids

The *trans* isomers of fatty acids were determined in the oil extracts as their methyl esters by gas chromatography. The prepara-

tion of fatty acid methyl esters (FAME) was accomplished using methanolic NaOH (2 mol/l) and methanolic HCL (1 mol/l). Quantitative analysis of FAME was performed with a gas chromatograph (Perkin–Elmer, Autosystem XL) equipped with a flame ionisation detector (FID). A BPX 90 capillary column (30 m length × 0.25 mm i.d. × 0.25 μm film thickness) from SGE was used. The temperature program was as follows: initial temperature, 145 °C (1 min holding), raised to 170 °C at 10 °C/min, and was hold for 10 min, before raising further up to 230 °C at 15 °C/min, then isothermal for 4 min. Injector and detector temperatures were 270 and 280 °C, respectively. The carrier gas was hydrogen at a flow rate of 0.7 ml/min.

2.3. Front-face fluorescence measurements

Fluorescence landscapes were measured directly on the samples without any prior treatment except grinding for nuts. EEMs were measured with a Varian Eclipse Fluorescence Spectrometer equipped with a Xenon lamp source, excitation and emission monochromators and a front-face sample cell holder. The settings for the instrument were: slit widths 5 nm (for both excitation and emission), emission wavelengths 280–700 nm (recorded every 2 nm), excitation wavelengths 280–600 nm (recorded every 8 nm), and scan rate 1200 nm/min. A PMT detector voltage of 550 V was used. All samples were analysed in triplicate on different sides of the cuvette.

2.4. Data processing

2.4.1. PARAFAC

PARAFAC models were developed for nuts (data array with 24 samples, 40 excitation wavelengths and 205 emission wavelengths) and sesame seeds (data array with 57 samples, 40 excitation wavelengths and 205 emission wavelengths) separately. Because of computational problems the emission dimension was reduced to the half giving a final data matrix of $24 * 40 * 103$ and $57 * 40 * 103$ for nuts and sesame seeds, respectively. PARAFAC models with 1–6 components were calculated, using the N-way toolbox5. Non negativity constraint was applied in all 3 modes. All the data in the EEM where the emission is lower than the excitation wavelength was set to zero. Zero values were also inserted in the area covered by the 2nd order Rayleigh scatter line. Missing values were inserted in the area covered by the 1st order Rayleigh scatter line giving a total of 4.85% of missing values, according to the method of Thygesen, Rinnan, Barsberg, and Møller (2004). The algorithms for the insertion of zeros and missing values were written in-house. The core consistency diagnostic was used as a measure of percentage of agreement of the PARAFAC models with ideal trilinearity. The number of PARAFAC factors to retain and the validity of the models were assessed through the residual analysis, the appropriateness of the spectral decomposition parameters and the core consistency value. Split-half analysis of PARAFAC models was also performed for validation. The idea of this strategy is to divide the data set into two halves and make a PARAFAC model on both halves. Due to the uniqueness of the PARAFAC model, one will obtain the same result – same loadings in the non-split mode, e.g., excitation and emission mode – on both data sets, if the correct number of components is chosen. The split-half test, based on replicated samples, i.e., not splitting of the repetitions, was performed by calculating PARAFAC models for each half of the data set at a time, subsequently comparing the results and ensuring that more or less identical excitation and emission loadings were obtained.

2.4.2. CML and trans fatty acids calibration

Regression models (MLR and PLS) for nuts and sesame seeds were performed between conventionally determined CML and tFA content and the scores of the PARAFAC factors. Leave-one-out cross validation was applied throughout this study and only validated results are presented. Correlation coefficient (R) and prediction error expressed as root mean square error of cross-validation (RMSECV) were used to evaluate the regression models quality. Also, PLS regression over chemical indicators values was performed on unfolded fluorescence emission spectra.

2.4.3. Oxidation prediction

To investigate whether fluorescence is able to predict the oxidative status of the samples, MLR models were constructed between PARAFAC scores and content of hydroperoxides and aldehydes (pAV and TBARS) in both nuts and sesame seeds.

2.5. Software

Data analyses were performed in MatLab Software (version 7) with the N-way Toolbox and the PLS Toolbox 3.5. In the N-way Toolbox, missing values in the PARAFAC modelling are handled by expectation maximization. No pre-processing of the data was used in PARAFAC. Scaling was performed on the unfolded spectra prior to PLS modeling.

3. Results and discussion

3.1. Modifications in the fluorescence fingerprint after processing

The fluorescence landscapes of two almond samples (a: before roasting and b: after roasting) are given in Fig. 1. The two landscapes express very marked differences in fluorescence shape and intensity. The highest fluorescent peak for the raw sample is at excitation 290 nm and emission around 330 nm. These fluorescence characteristics correspond to tryptophan and tocopherols, which are both expected to be present in almonds. This fluorescence emission considerably decreased in the roasted sample. Furthermore, a broad fluorescence band probably corresponding to various fluorophores with excitation maximum around 370 nm and emission maximum around 450 nm appear during roasting. These fluorescent molecules could be associated to NFC arising consecutively to the thermal process.

In Fig. 1, the fluorescence landscapes of sesame seed samples during roasting (a: before roasting, and after b: 30 min, c: 75 min, d: 120 min of roasting) clearly show the progressive development of a fluorescence zone with excitation/emission maxima around 360/450 nm as a function of roasting time. Again, this neoformed fluorescence could be attributed to the heat generated neoformed compounds.

This fluorescence zone corresponds fairly well to heat oxidation products described in the literature (Christensen, 2005). It resembles the fluorophores present in refined oils and the oxidation production derived upon thermal treatment (Sikorska et al., 2004). The same fluorescence was also evidenced to appear in roasted soya proportionally to the heating time, when lipids were present (Birlouez-Aragon et al., 2001). Previous delipidation of the soya before roasting dramatically impeded the formation of this fluorescence (Birlouez-Aragon et al., 2001). We therefore assign this fluorescence in processed nuts and sesame seeds to Maillard products formed between proteins and lipidic secondary aldehydes.

3.2. PARAFAC results

The aforementioned patterns in the fluorescence landscapes were investigated further by the use of PARAFAC analysis with the objective to resolve the fluorescence signal into individual contributions of fluorescence profiles varying linearly in intensity

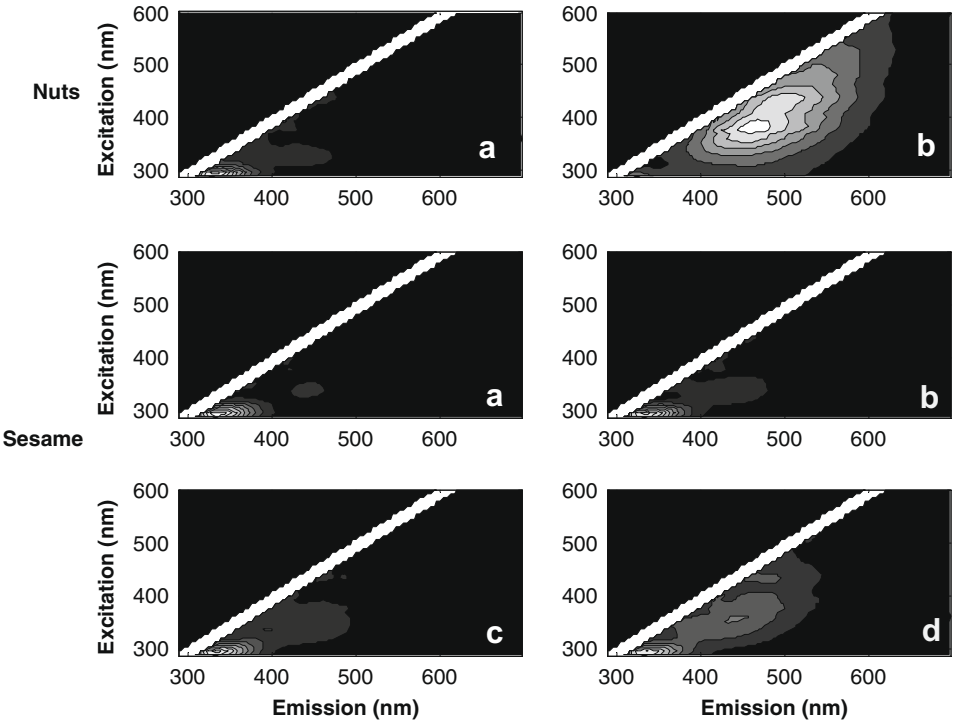

Fig. 1. Contour plot of a fluorescence landscape of almond samples (a) raw almond sample and (b) roasted almond sample, and sesame seed samples (a) Raw sample, (b) 30 min roasted sample, (c) 75 min roasted sample, and (d) 120 min roasted sample. White indicates the maximum fluorescence intensity. The diagonal white band holds 1st order Rayleigh scatter signal treated as missing values.

amongst the samples. The modes 2 and 3 obtained by the PARAFAC decomposition allow describing the emission and excitation profiles of each factor corresponding to homogenous fluorescence profiles composing the three-dimensional fluorescence landscapes.

3.2.1. PARAFAC modelling in nuts

PARAFAC models on fluorescence landscapes of nuts were estimated with one to six factors and compared. Based on core consistency, split-half validation and visual inspection of both the residuals and the loadings, the PARAFAC model with four components, i.e., four different fluorescence profiles, was considered optimal (explained variance 96.6%, core consistency value 84.5) in nuts. The scores (mode 1) and emission/excitation plots (mode 2 and 3) are shown in Fig. 2. The components are displayed in the same order as they are modelled, depending on their contribution to the sample profiles. The excitation and emission maxima of the four PARAFAC components are illustrated in Fig. 2a and b. The 332 nm emission maximum is easily identified in the raw data (Fig. 2), and was attributed to tryptophan and tocopherols, whilst the 444, 488 and 544 nm emission maxima are a part of the broad emission evidenced in the raw data as neoformed fluorescence (Fig. 1). The intensity of these four PARAFAC components can be followed in the score plots (Fig. 2c and d), displaying the distribution of the samples. The score values are plotted in order to easily describe the fluorophores development throughout the processing stages. Thus, tryptophan and tocopherol fluorescence (factor 3) in almonds (c) and peanuts (d) decreased after roasting, whereas the development in NFC fluorescence globally increased immediately after roasting.

3.2.2. PARAFAC modelling in sesame seeds

PARAFAC decomposition of sesame seeds and Tahina fluorescence landscapes was calculated using one to six factors. Based on the same evaluation tools as described before, the PARAFAC model with five components was considered optimal (explained variance 98.3%, core consistency value 52). The scores and loading plots are shown in Fig. 3. The components are displayed in the same order as they are modelled, depending on their contribution to the sample profiles. The intensity of the five PARAFAC components can be followed in the score plots (Fig. 3c and d), displaying the distribution of the samples. In Tahina, similarly as in nuts (Fig. 3c), tryptophan and tocopherol fluorescence decreased throughout the processing steps, whereas NFC fluorescence continuously increased during roasting, except component three with excitation/emission maxima (336/380 nm) which firstly increased till the beginning of roasting and decreased in the late stages of roasting. The same observations were done for sesame seeds roasting (Fig. 3d): NFC fluorescence increased, mainly after 60 min for components 2–4, and 75 min for component 5, with a decrease for component three after 90 min of roasting. This suggests that component 3 is associated with early oxidation and/or Maillard products that decrease as a result of their degradation into more advanced products or due to their reaction with other food constituents, particularly proteins.

The excitation/emission maxima found for the PARAFAC loadings for the models of nuts and sesame seeds are quite similar with small shifts probably due to differences in the physicochemical structure of the various food matrices. We hypothetize that the one extra component at exc/em (336/380 nm) found as transitory fluorescence in sesame seeds but not in nuts could be detected thanks to the small interval sampling performed during the roasting of sesame seeds.

Thus, the results from PARAFAC decomposition applied on both nuts and sesame seeds allowed monitoring the changes in fluorophores that occurred during processing. The decrease in tocopherol fluorescence during roasting is probably due to quenching by absorbing substances formed during lipid peroxidation (aldehydes absorbing at 260–280 nm) (Rovellini, Cortesi, & Fedeli, 1997). Another hypothesis has been suggested to explain such decrease in tryptophan fluorescence. Heat treatment causes partial

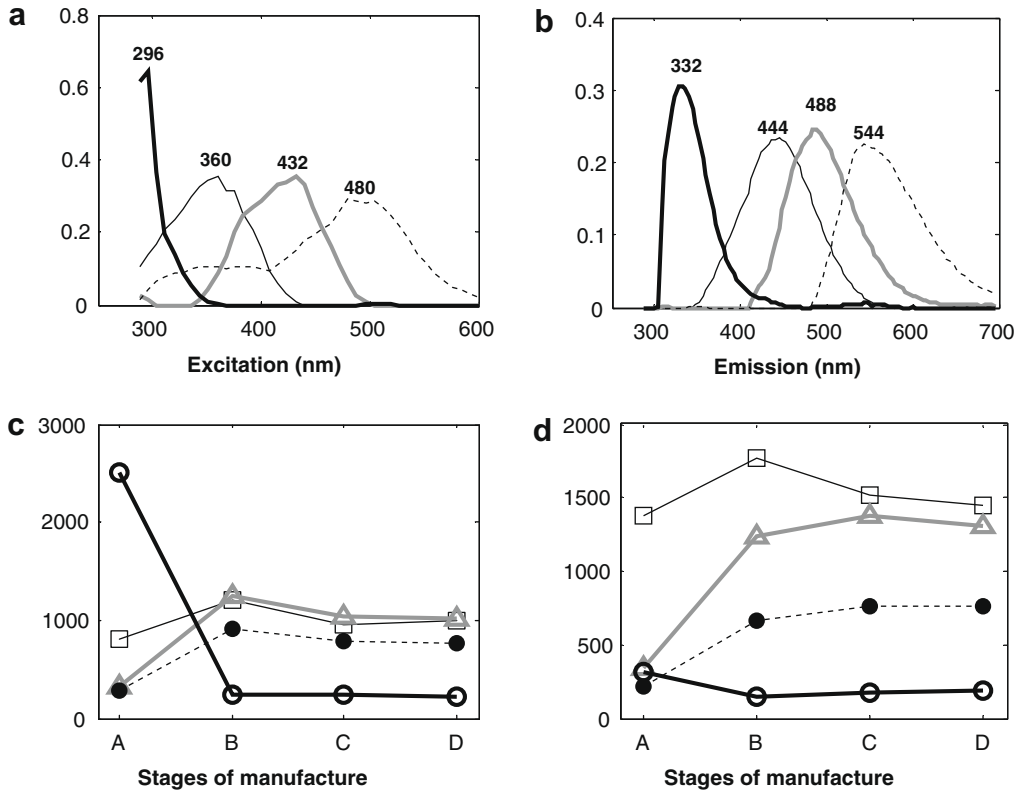

Fig. 2. (a) excitation loadings, (b) emission loadings, (c) scores of almond samples, and (d) scores of peanut samples, of a four component PARAFAC model, based on the fluorescence landscapes of 24 roasted nut samples. Excitation and emission maxima (nm) of each component are displayed. Factor 1 (thin black line), factor 2 (grey line), factor 3 (thick black line), factor 4 (dotted line).

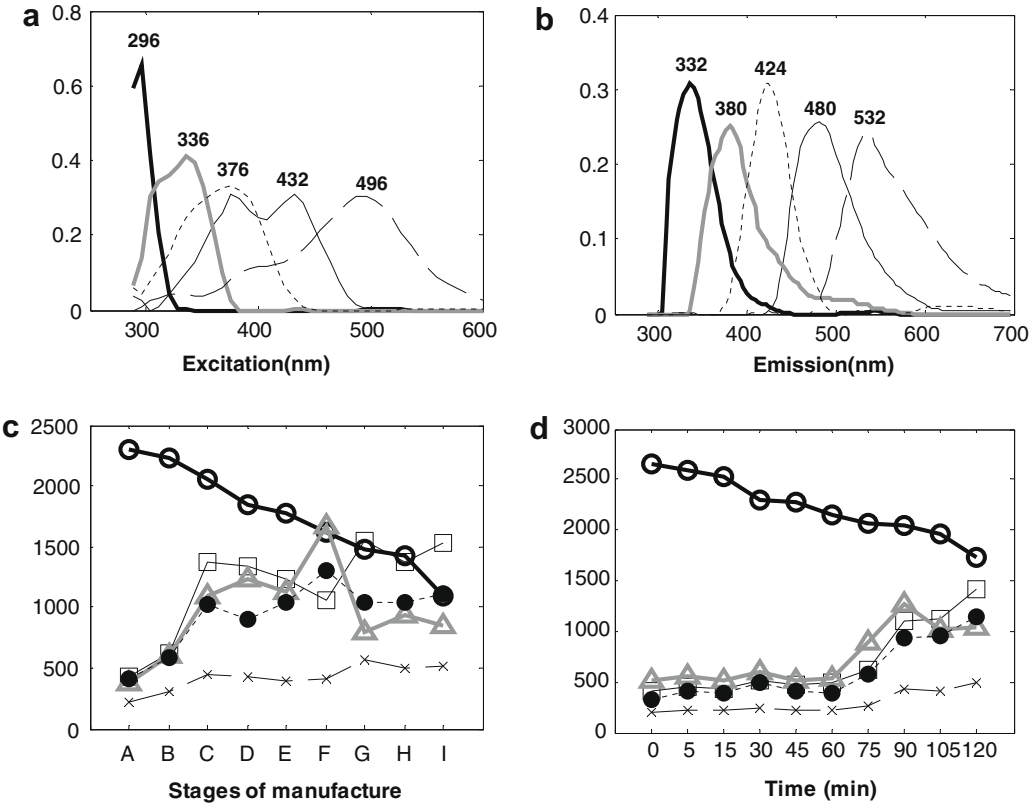

Fig. 3. (a) excitation loadings, (b) emission loadings, (c), scores of Tahina samples, and (d) scores of roasted sesame seed samples, of a five component PARAFAC model, based on the fluorescence landscapes of 57 sesame seed samples. Excitation and emission maxima (nm) of each component are displayed. Factor 1 (thick black line), factor 2 (thin black line), factor 3 (grey line), factor 4 (dotted line), factor 5 (dashed line).

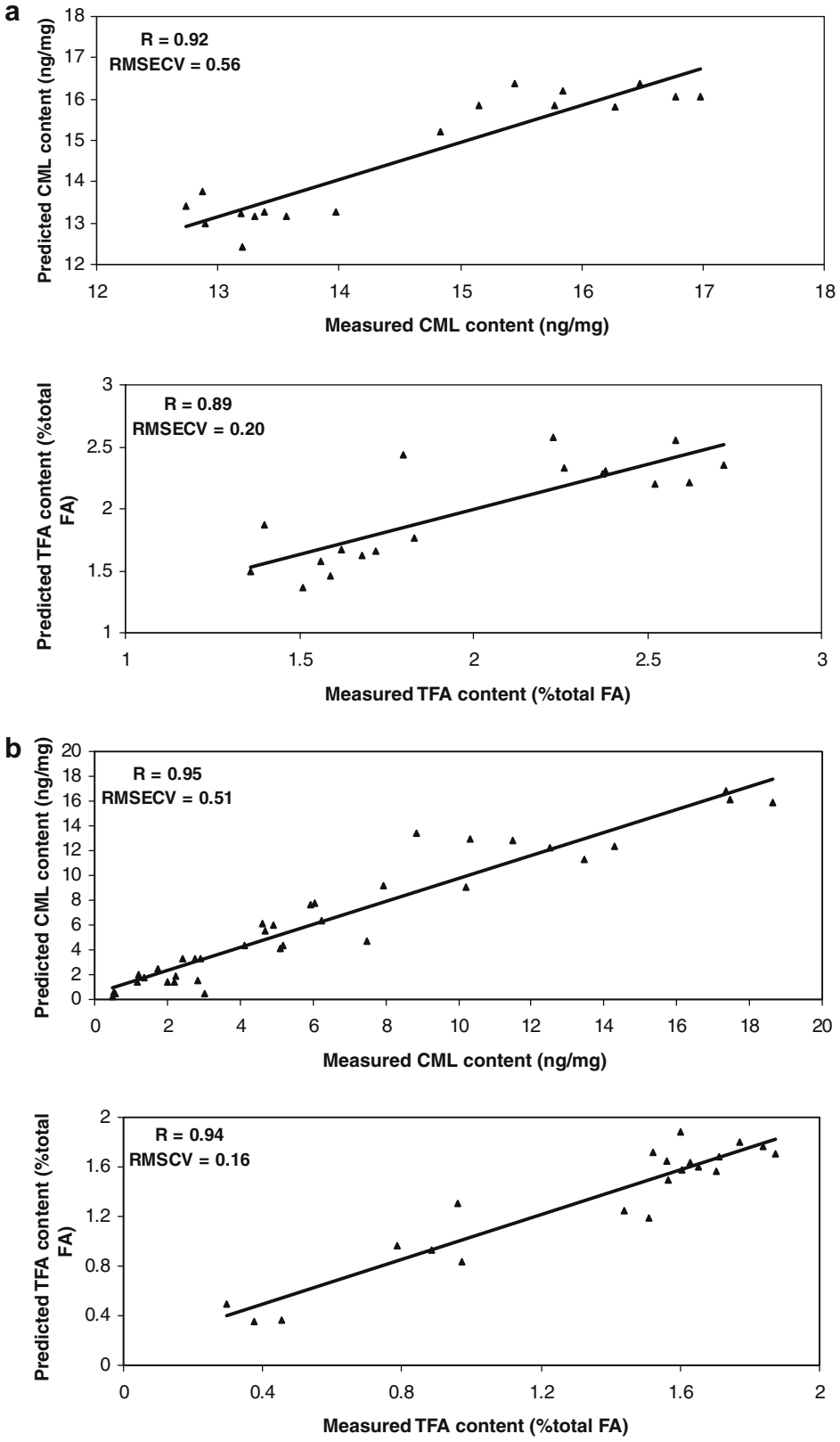

Fig. 4. Predicted versus measured CML and tFA content of (a) nuts and (b) sesame seeds, based on MLR model on PARAFAC scores. The correlation coefficient (*R*) and prediction error (RMSECV) are reported.

denaturation of proteins and formation of fluorescent Maillard reaction products. As a consequence of the denaturation, part of the tryptophan environment in the proteins is modified resulting in a decreased tryptophan quantum yield (Dufour & Riaublanc, 1997). The decrease in tryptophan fluorescence could be also due to reabsorption by NFC appearing in the roasted samples and absorbing in the tryptophan emission range (330–360). The observed increase at excitation/emission around 360–370/450 nm is

very probably due to reported reactions of malondialdehyde or other lipid derived aldehydes with amino compounds which develop during the heat treatment under aerobic conditions (Kikugawa & Beppu, 1987; Wold & Mielnik, 2000), indicating increased level of lipid oxidation (Hasegawa et al., 1992). Finally, an increase in the fluorescence emission 530–540 nm was also observed in cookies as appearing during baking (Ait Ameur, 2006). No hypothesis on the molecular structure of such fluorophores was proposed, but we suppose from the late appearance of this last fluorescence during the heat treatment that it should be associated to late stage lipid–protein adducts.

3.3. CML and tFA calibration

To verify the correlation between CML and fluorescence signal, various regression models were developed. At first, the score values of the PARAFAC components were compared with the conventional determined CML content. MLR was applied to the obtained PARAFAC score vectors (mode 1) in order to predict CML concentrations in nuts and sesame seeds. Regression models employing one of the components at a time show that PARAFAC component 1 in nuts and 4 in sesame seeds, i.e. the fluorescence at (360–375)/(424–440) contributes most to the prediction ability of CML for the nuts ($R = 0.85$) and sesame seeds ($R = 0.93$), confirming the assignment of this PARAFAC component to fluorescent Maillard products formed with similar kinetics as CML. A negative correlation also exists between CML and the fluorescence at 296/332 in both nuts ($R = 0.73$) and sesame seeds ($R = 0.72$). However, the results indicate that the regression model for predicting the CML content from the fluorescence landscapes is optimised by including the other PARAFAC scores in the regression model. Results are shown in Table 1 and Fig. 4. The 4-component PARAFAC model generated from nut samples provided a good correlation ($R = 0.92$) with a prediction error (RMSECV) of 0.56 ng/mg, corresponding to 3.8% of the mean CML content in the nut samples. The 5-component PARAFAC model generated from sesame seed samples provided also a good correlation ($R = 0.95$) with a prediction error (RMSECV) of 0.51 ng/mg, corresponding to 8.2% of the mean CML content in the sesame seed samples. The lower predictive performance of the sesame seeds model compared to the nuts model could be explained by a sample set covering a larger CML concentration area, from 0.5 to 18.6 ng/mg. Thus, by comparing the relative prediction errors in percent calculated as RMSECV/range, we obtain similar performances for the 2 models estimating the CML (13 and 14% in nuts and sesame seeds, respectively).

Similarly, MLR was applied to the obtained PARAFAC score vectors (mode 1) in order to predict tFA concentrations in nuts and sesame seeds. Regression models employing one of the components at a time show that PARAFAC component 4 in nuts and 5 in sesame seeds, i.e., the fluorescence at (480–496)/(532–544), contribute most to the prediction ability of tFA ($R = 0.82$) for both nuts and sesame seeds, which means that tFA, generally associated with severe heat treatment, correlate well with the more advanced oxidation products that fluoresce in this zone. The 4-component PARAFAC model generated from nut samples provided a good correlation ($R = 0.89$) with a prediction error (RMSECV) of 0.2% of total fatty acids (FA), corresponding to 10% of the mean tFA content in the nuts samples (Table 1, Fig. 4a). The 5-component PARAFAC model generated from sesame seed samples provided also a good correlation ($R = 0.94$) with a prediction error (RMSECV) of 0.16% of total FA, corresponding to 12% of the mean tFA content in the sesame seed samples (Table 1, Fig. 4b).

In Table 1, the results of different regression models for both CML and tFA are compared based on the correlation coefficients (R), calibration (RMSEC) and prediction (RMSECV) errors. Comparing MLR on PARAFAC scores with PLS regression on PARAFAC scores as well as on unfolded fluorescence spectra in both nuts and sesame seeds, allowed evidencing that PLS regression models performed significantly weaker (higher RMSECV values), compared with the best performing regression MLR model on PARAFAC scores. At the calibration stage also, the MLR model shows the lowest values for RMSEC. This indicates that the MLR model also fits the data optimally.

3.4. Front-face fluorescence in the monitoring of oxidation

Univariate correlations between PARAFAC components and reference measurements of lipid oxidation showed that TBARS and *p*AV are mainly correlated with the PARAFAC component associated with the fluorescence at 360/440 in both nuts and sesame seeds, confirming assignment of this PARAFAC component to products from reactions of secondary aldehydic oxidation products with peptide amino groups.

The results of the calculated MLR models on PARAFAC scores are listed in Table 2. They clearly show that prediction of oxidation by fluorescence results in the highest correlations for sesame seeds when using this specific fluorescence ($R = 0.96$; RMECV = 10 and 8%, respectively). For nuts, models performed poorer, with prediction errors of 22 and 19% for *p*AV and TBARS respectively. In the conditions used in this study, hydroperoxides were only formed

Table 1
Results from different regression models on CML and tFA content of nuts and sesame seed samples.

Data set	Method	# Comp[a]	R^2[b]	RMSEC[c]	RMSECV[d]	Y-mean [e]	Y-range [f]
Nuts (CML) $N = 18$	MLR on PARAFAC scores 1–4	4	0.92	0.40	0.56	14.6	12.7–16.9
	PLSR on PARAFAC scores 1–4	2	0.91	0.59	0.67		
	PLSR on unfolded emission spectra	3	0.87	0.72	0.92		
Nuts (tFA) $N = 18$	MLR on PARAFAC scores 1–4	4	0.89	0.18	0.20	2	1.3–2.7
	PLSR on PARAFAC scores 1–4	2	0.86	0.22	0.26		
	PLSR on unfolded emission spectra	2	0.78	0.28	0.31		
Sesame seeds (CML)	MLR on PARAFAC scores 1–5	5	0.95	1.23	0.51	6.2	0.5–18.6
$N = 36$	PLSR on PARAFAC scores 1–5	3	0.95	1.31	1.48		
	PLSR on unfolded emission spectra	3	0.94	1.39	1.67		
Sesame seeds (tFA)	MLR on PARAFAC scores 1–5	5	0.94	0.12	0.16	1.3	0.3-1.8
$N = 21$	PLSR on PARAFAC scores 1–5	2	0.90	0.20	0.22		
	PLSR on unfolded emission spectra	2	0.91	0.20	0.24		

[a] Optimal number of components in the model.
[b] Correlation coefficient.
[c] Root mean square error of calibration, expressed in ng/mg for CML and % of total FA for tFA.
[d] Root mean square error of cross-validation, in ng/mg for CML and % of total FA for tFA.
[e] Mean concentration in the sample set, expressed in ng/mg for CML and % of total FA for tFA.
[f] Range of the concentration in the sample set, expressed in ng/mg for CML and % of total FA for tFA.

Table 2
Results from MLR models between PARAFAC scores and oxidation determinants of nuts and sesame seed samples.

Data set		# Comp[a]	R^2[b]	RMSEC[c]	RMSECV[d]	Y-mean	Y-range
Nuts $N = 24$	*p*Av	4	0.73	0.64	0.78	6.03	4.3–7.8
	Hydroperoxydes	4	0.52	0.34	0.8	1.47	0.07–3.15
	TBARS	4	0.73	0.54	0.66	2.82	1.2–4.6
Sesame seeds $N = 30$	*p*AV	5	0.96	0.15	0.18	7.5	6.8–8.6
	Hydroperoxydes	5	0.70	0.31	0.39	2.6	1.6–3.5
	TBARS	5	0.96	0.05	0.06	2.17	1.8–2.5

[a] Optimal number of components in the model.
[b] Correlation coefficient in prediction.
[c] Root mean square error of calibration.
[d] Root mean square error of cross validation.

transitorily (data not shown). Consequently, there was no good correlation found between hydroperoxide concentrations and fluorescence spectra. The correlations obtained between TBARS and fluorescence were similar to those reported by others on meat products (Wold et al., 2002; Gatellier et al., 2007). A satisfactory correlation ($R2 = 0.73$) was also found between free radicals, an indicator of early oxidation, and fluorescence landscapes in peanuts (Jensen et al., 2004). These results show that fluorescence spectra associated with PARAFAC decomposition could be used to monitor the oxidative degradation of nuts and sesame seeds during their processing.

4. Conclusion

This exploratory study was dedicated at demonstrating the potential of fluorescence spectroscopy in combination with chemometrics for monitoring of lipid oxidation and NFC during nuts and sesame seeds processing. The technique appears highly satisfactory with prediction errors lower than 10% in most cases. Moreover, this innovative method is fast and nondestructive and could be applied online to control the roasting process. The fluorometric analysis reveals information about the molecular changes occurring in these food products when exposed to heat treatment. PARAFAC analysis provides a unique mathematical decomposition of four fluorescent compounds present in nuts and five in sesame seed samples, all showing a change in the fluorescence signal throughout the processing stages. Front-face fluorescence spectroscopy appears a very sensitive technique for determining lipid oxidation products, as well as CML and tFA in nuts and sesame seeds. Whereas the determination of CML content from the fluorescence spectra can be explained by indirect correlation with the fluorescence of advanced Maillard products emitting in the 420–440 nm region, the correlation between the fluorescence spectra at 520 nm and the tFA content is more difficult to explain.

We can hypothesise that tFA and fluorophores emitting at 520 nm are formed with parallel kinetic rates during nut and seed roasting.

Acknowledgement

This work was supported by a Grant from the Lebanese National Council for Scientific Research.

References

Ait Ameur, L. (2006). Evolution de la qualité nutritionnelle des protéines de biscuits modèles au cours de la cuisson au travers d'indicateurs de la réaction de Maillard: intérêt de la fluorescence frontale. PhD thesis, Institut National Agronomique Paris Grignon, France (http://pastel.paristech.org/2269).

Aubourg, S. P. (1999). Recent advances in assessment of marine lipid oxidation by using fluorescence. *Journal of the American Oil Chemists' Society, 76*(4), 409–419.

Birlouez-Aragon, I., Leclère, J., Ouedraogo, C. L., Birlouez, E., & Grongnet, J. F. (2001). The fast method, a rapid approach of the nutritional quality of heat-treated foods. *Nahrung/Food, 45*(3), 201–205.

Birlouez-Aragon, I., Locquet, N., De St Louvent, E., Jouan-Rimbaud Bouveresse, D., & Stahl, P. (2005). Evaluation of the Maillard reaction in infant formulas by means of front face fluorescence. *Annals of the New York Academy of Sciences, 1043*, 308–318.

Birlouez-Aragon, I., Mas, P. A., Ait Ameur, L., Locquet, N., De St Louvent, E., & Zude, M. (2004). Fluorescence fingerprints as a rapid predictor of the nutritional quality of processed and stored foods. *Czech Journal of Food Science, 22*, 68–71.

Buedge, J. A., & Aust, S. D. (Eds.). (1978). *Microsomal lipid peroxidation* Fleisher, S. F., & Packer, L. (Eds.). *Biomembranes (Part C: Biological oxidation) methods in enzymology* (Vol. 52, pp. 302–309). London: Academic Press.

Charissou, A., Ait-Ameur, L., & Birlouez-Aragon, I. (2007). Evaluation of a gas chromatography/mass spectrometry method for the quantification of carboxymethyllysine in food samples. *Journal of Chromatography A, 1140*(1–2), 189–194.

Cheikhousman, R., Zude, M., Jouan-Rimbaud Bouveresse, D., Léger, C., Rutledge, D., & Birlouez-Aragon, I. (2005). Fluorescence spectroscopy for monitoring deterioration of extra virgin olive oil during heating. *Analytical and Bioanalytical Chemistry, 382*, 1438–1443.

Christensen, J. (2005). Autofluorescence of intact food – an exploratory multiway study. PhD thesis, The Royal Veterinary and Agricultural University, Denmark.

Christensen, J., Povlsen, V. T., & Sorensen, J. (2003). Application of fluorescence spectroscopy and chemometrics in the evaluation of processed cheese during storage. *Journal of Dairy Science, 86*, 1101–1107.

Dufour, E., & Riaublanc, A. (1997). Potentiality of spectroscopic methods for the characterization of dairy products. II-Mid infrared study of the melting temperature of cream triacylglycerols and of the solid fat content in cream. *Lait, 77*(6), 671–681.

Engelsen, S. B. (1997). Explorative spectrometric evaluations of frying oil deterioration. *Journal of the American Oil Chemists Society, 74*(12), 1495–1508.

Esterbauer, H., Koller, E., Slee, R. G., & Koster, J. F. (1986). Possible involvement of the lipid-peroxidation product 4-hydroxynonenal in the formation of fluorescent chromolipids. *Biochemical Journal, 239*, 405–409.

Gatellier, P., Gomez, S., Gigaud, V., Berri, C., Le Bihan-Duval, E., & Santé-Lhoutellier, V. (2007). Use of a fluorescence front face technique for measurement of lipid oxidation during refrigerated storage of chicken meat. *Meat Science, 76*, 543–547.

Genot, C. (1996). Some factors influencing TBA test. In Report of diet-ox project (AIRIII-CT-92-1577).

Hasegawa, K., Endo, Y., & Fujimoto, K. (1992). Oxidative detoriation in dried fish model systems assessed by solid sample fluorescence spectrophotometry. *Journal of Food Science, 57*, 1123–1126.

Jensen, J. N., Christensen, J., & Engelsen, S. B. (2004). Oxidative changes in in pork scratchings, peanuts, oatmeal, and muesli viewed by fluorescence, near-infrared and infrared spectroscopy. *European Food Research Technology, 219*, 294–304.

Jiang, Z. E., Woollard, A. C. S., & Wolff, S. P. (1990). Lipid hydroperoxide measurement by oxidation of Fe^{2+} in the presence of xylenol orange. Comparison with the TBA assay and an iodometric method. *Lipids, 26*(10), 853–856.

Kikugawa, K., & Beppu, M. (1987). Involvement of lipid oxidation products in the formation of fluorescent and cross linked proteins. *Chemistry and Physics of Lipids, 44*, 277–296.

Kulmyrzaev, A., & Dufour, E. (2002). Determination of lactulose and furosine in milk using front-face fluorescence spectroscopy. *Lait, 82*, 725–735.

Liang, J. H. (2000). Kinetics of fluorescence formation in whole milk powders during oxidation. *Food Chemistry, 71*, 459–463.

Melton, S. L. (1983). Methodology for following lipid oxidation in muscle food. *Food Technology, 37*, 105–111.

Moller, J. K. S., Parolari, G., Gabba, L., Christensen, J., & Skibsted, L. H. (2003). Monitoring chemical changes of dry-cured parma ham during processing by surface autofluorescence spectroscopy. *Journal of Agricultural and Food Chemistry, 5*(5), 1224–1230.

Olsen, E., Vogt, G., Veberg, A., Ekeberg, D., & Nilsson, A. (2005). Analysis of early lipid oxidation in smoked, comminuted pork or poultry sausages with spices. *Journal of Agriculture and Food Chemistry, 53*, 7448–7457.

Rizkallah, J., Lakhal, L., & Birlouez-Aragon, I. (2008). Front-face fluorescence analysis to monitor food processing and neoformed contamination. In M. Zude (Ed.), *Optical monitoring of fresh and processed agricultural crops*. USA: CRC Press.

Rovellini, P., Cortesi, N., & Fedeli, E. (1997). Ossidazioni dei lipidi. Nota 1. *La Rivista Italiana delle Sostanze Grasse, 74*(5), 181–189.

Sikorska, E., Romaniuk, A., Khmelinskii, I. V., Herance, R., Bourdelande, J. L., Sikorski, M., & Koziol, J. (2004). Characterization of edible oils using total luminescence spectroscopy. *Journal of Fluorescence, 14*(1), 25–35.

Thygesen, L. G., Rinnan, A., Barsberg, S., & Møller, J. K. S. (2004). Stabilizing the PARAFAC decomposition of fluorescence spectra by inserting zeros outside the data area. *Chemometrics and Intelligent Laboratory systems, 71*, 97–106.

Wold, J. P., & Mielnik, M. (2000). Nondestructive assessment of lipid oxidation in minced poultry meat by autofluorescence spectroscopy. *Journal of Food Science, 65*, 87–95.

Wold, J. P., Mielnik, M., Pettersen, M. K., Aaby, K., & Baardseth, P. (2002). Rapid assessment of rancidity in complex meat products by front face fluorescence spectroscopy. *Journal of Food Science, 67*, 2397–2404.